THE INVERSE KINEMATICS AND DYNAMICS OF A FLEXIBLE MANIPULATOR FOR TRAJECTORY AND FORCE CONTROL

Katsuyoshi Tsujita, Kazuo Tsuchiya, Toshio Kamiya and **Yousuke Kawano**
Dept. of Aeronautics and Astronautics,
Graduate School of Engineering, Kyoto University,
E-mail: tsujita@space.kuaero.kyoto-u.ac.jp
tsuchiya@space.kuaero.kyoto-u.ac.jp

ABSTRACT
This paper deals with an inverse model of a planar manipulator with two links, one rigid link and the other is elastic. The model of the inverse kinematics and the inverse dynamics for a trajectory and force control of the manipulator is proposed. In the model, the equations for the elastic deformations of the elastic link are formulated as boundary value problems. The model proposed does not include any iteration processes. The accuracy of the model is checked numerically.

INTRODUCTION
Many researches on motion control of mechanical systems composed of rigid and elastic bodies have been proposed so far. One basic method to control the motion of a non-linear mechanical system is the computed torque method. The computed torque method is composed of two steps. The first step is called inverse kinematics; When some state variables of the system are given as functions of time, it is to calculate the values of the rest state variables of the system. The second step is called inverse dynamics; When the motion of the system is given, control forces(torques) to actuators are calculated to realize the given motion. As the models for the inverse dynamics, dynamic equations are used. And the inputs are the state variables as time functions and outputs are the control forces (torques). On the other hand, the models for the inverse kinematics are generally derived from the kinetic equations of the system. But, there are some systems in which the basic equations can't be derived from only the kinetic equations. A mechanical system composed of rigid and elastic bodies is a typical example of this class of mechanical system. In this case, we have to derive the models by using dynamic equations as well as kinetic ones. So, the basic problems of the inverse kinematics of this class of mechanical system is how to derive the model by using kinetic and dynamic equations and how to solve it ([1] $\sim$ [5]).

In this paper, we will take up a planar two-link manipulator with a force sensor on the end effector as one example of this class of mechanical system. The first link of the manipulator is a rigid link and the other is composed of a elastic beam and rigid ome. We proposed a model and an algorithm of the inverse kinematics and dynamics of the system for trajectory and force control. The dynamic equations of the system are derived by the use of the D'Alembert principle where the motion of the second and third links are modeled by the finite element method. The models of the inverse kinematics are derived by the dynamic equations of the system and the kinetic equation of the end effector where the inputs are the trajectory of the end effector and the force acting on the end effector and outputs are the trajectory of the joints and the vibrations of the second link. The crucial point of the model is that since the equations of the elastic vibration of the second link become to be ill-posed as the initial value problems they are reformulated as the boundary value problems. The algorithm based on the model does not involve any iteration processes. The model of the inverse dynamics are derived by dynamic equations of the system where the inputs are the motion of the system and the outputs are the torques of the motors installed at the joints. In this case, since the models of the inverse dynamics have no solutions, the torques of the motors are given as solutions of the models with the least squared errors.
Numerical simulations are implemented to verify the efficiency of the proposed model and algorithm.

EQUATIONS OF MOTION
Consider a manipulator composed of two links, link 1, 2 (Figure 1). Link 1 is put on a base with a rotary joint (joint 1) , link 2 is connected to link 1 with a rotary joint (joint 2). Link 1 is a rigid rod and link 2 is composed of a elastic beam and a rigid part. A rigid part of link 2 is connected to the elastic part with a rotary joint (joint 3). Motors are installed

at the rotary joint 1,2 and 3, the axes of which are perpendicular to a vertical plane. Motors of joint 1 and 2 generate control torques to control the trajectory of the manipulator. On the other hand, the motor of joint 3 acts as a rotary passive compliance and also is able to generate control torque to control the force acting on the end effector. The elastic deformations of link 2 occur in a plane perpendicular to the axis of rotation. Introduce a set of unit vectors $\{\boldsymbol{a}^{(0)}\} = \{\boldsymbol{a}_1^{(0)}, \boldsymbol{a}_2^{(0)}, \boldsymbol{a}_3^{(0)}\}$ fixed in an inertia space, the origin of which coincides with joint 1. Vector $\boldsymbol{a}_3^{(0)}$ coincides with the axis of rotation and vector $\boldsymbol{a}_2^{(0)}$ is set downward. A set of unit vectors $\{\boldsymbol{a}^{(i)}\} = \{\boldsymbol{a}_1^{(i)}, \boldsymbol{a}_2^{(i)}, \boldsymbol{a}_3^{(i)}\}$ $(i = 1, 2)$ is introduced, the origin of which coincides with joint i. Vector $\boldsymbol{a}_3^{(i)}$ coincides with the axis of rotation of joint i and vector $\boldsymbol{a}_1^{(i)}$ is set toward the axis of link i. Using a set of unit vectors $\{\boldsymbol{a}^{(i)}\}$, a column matrix is introduced,

$$[\boldsymbol{a}^{(i)}]^T = [\boldsymbol{a}_1^{(i)}, \boldsymbol{a}_2^{(i)}, \boldsymbol{a}_3^{(i)}] \tag{1}$$

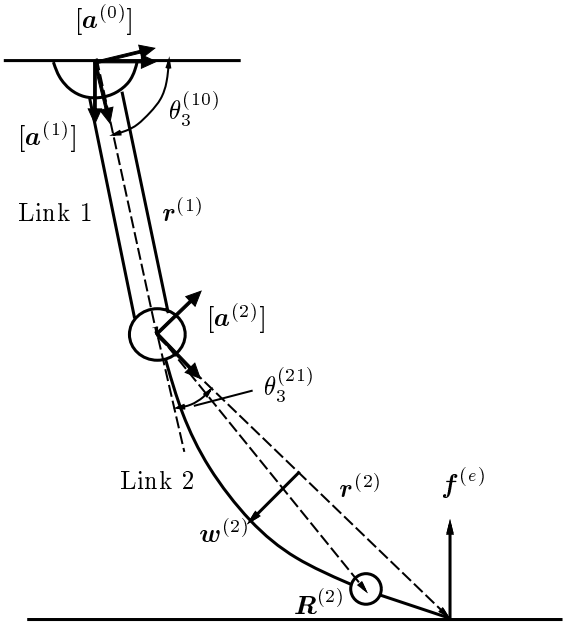

FIGURE 1: Two link manipulator system

A transformation matrix from $\{\boldsymbol{a}^{(j)}\}$ to $\{\boldsymbol{a}^{(i)}\}$ is defined by $A^{(ij)}(i, j = 0, 1, 2)$

$$\begin{aligned} [\boldsymbol{a}^{(i)}] &= A^{(ij)}[\boldsymbol{a}^{(j)}] \\ A^{(ij)} &= \begin{bmatrix} \cos\theta_3^{(ij)} & \sin\theta_3^{(ij)} & 0 \\ -\sin\theta_3^{(ij)} & \cos\theta_3^{(ij)} & 0 \\ 0 & 0 & 1 \end{bmatrix} \end{aligned} \tag{2}$$

where, $\theta_3^{(ij)}$ is angle of rotation from $\{\boldsymbol{a}^{(j)}\}$ to $\{\boldsymbol{a}^{(i)}\}$ about $\boldsymbol{a}_3^{(j)}$ axis.

The angular velocity vector of $\{\boldsymbol{a}^{(i)}\}$ to $\{\boldsymbol{a}^{(j)}\}$ is defined by $\boldsymbol{\omega}^{(ij)}$

$$\begin{aligned} \boldsymbol{\omega}^{(ij)} &= [\boldsymbol{a}^{(i)}]^T \omega^{(ij)} \\ \omega^{(ij)T} &= [0, 0, \dot{\theta}_3^{(ij)}] \end{aligned} \tag{3}$$

The following quantities are introduced,

$\boldsymbol{r}^{(1)} = [\boldsymbol{a}^{(1)}]^T r^{(1)}$; a distance vector from joint 1 to joint 2.

$\boldsymbol{r}^{(2)} = [\boldsymbol{a}^{(2)}]^T r^{(2)}$; a distance vector from joint 2 to the end effector.

$\boldsymbol{R}^{(2)} = [\boldsymbol{a}^{(2)}]^T R^{(2)}$; a distance vector from joint 2 to joint 3.

$\boldsymbol{\rho}^{(i)} = [\boldsymbol{a}^{(i)}]^T \rho^{(i)}$; a distance vector from joint i to any position in link i.

The elastic deformation of link 2 is denoted by $\boldsymbol{w}^{(2)}$

$$\begin{aligned} \boldsymbol{w}^{(2)} &= [\boldsymbol{a}^{(2)}]^T w^{(2)} \\ w^{(2)T} &= [0,\ w_2^{(2)}(t,\ \rho_1^{(2)}),\ 0] \end{aligned} \tag{4}$$

By using the finite element method, the elastic deformation $w_2^{(2)}(t,\ \rho_1^{(2)})$ is expressed as

$$w_2^{(2)}(t,\ \rho_1^{(2)}) = B^{(2)}(\rho_1^{(2)})\hat{w}_2^{(2)}(t) \tag{5}$$

Where the rigid part of link 2 is considered as one of the finite elements of link 2 as well as elastic part by selecting appropriate test functions corresponding to rigid mode.

A distance vector $\boldsymbol{x}^{(1)}$ from joint 1 to any point in link 1 is expressed as

$$\begin{aligned} \boldsymbol{x}^{(1)} &= [\boldsymbol{a}^{(1)}]^T x^{(1)} \\ x^{(1)} &= \rho^{(1)} \end{aligned}$$

and the velocity vector $\boldsymbol{v}^{(1)}$ is expressed as

$$\begin{aligned} \boldsymbol{v}^{(1)} &= [\boldsymbol{a}^{(1)}]^T v^{(1)} \\ v^{(1)} &= \tilde{\rho}^{(1)}\omega^{(10)} \end{aligned} \tag{6}$$

where,

$$\tilde{\rho}^{(1)} = \begin{bmatrix} 0 & \rho_3^{(1)} & -\rho_2^{(1)} \\ -\rho_3^{(1)} & 0 & \rho_1^{(1)} \\ \rho_2^{(1)} & -\rho_1^{(1)} & 0 \end{bmatrix}$$

On the other hand, a distance vector $\boldsymbol{x}^{(2)}$ from joint 1 to any point in link 2 is expressed as

$$\begin{aligned} \boldsymbol{x}^{(2)} &= [\boldsymbol{a}^{(2)}]^T x^{(2)} \\ x^{(2)} &= A^{(21)}r^{(1)} + (\rho^{(2)} + w^{(2)}) \end{aligned}$$

and the velocity vector $\boldsymbol{v}^{(2)}$ is expressed as

$$\begin{aligned} \boldsymbol{v}^{(2)} &= [\boldsymbol{a}^{(2)}]^T v^{(2)} \\ v^{(2)} &= A^{(21)}\tilde{\rho}^{(1)}\omega^{(10)} \\ &\quad + \{\tilde{\rho}^{(2)}\omega^{(20)} + B^{(2)}(\rho_1^{(2)})\dot{\hat{w}}^{(2)}(t)\} \end{aligned} \tag{7}$$

A state variable z of the system is set to be

$$z^T = [\theta_3^{(10)},\ \theta_3^{(21)},\ \hat{w}_2^{(2)T}] \tag{8}$$

The equations of motion for stable variable z are derived as follows; The equations for variables $\theta_3^{(10)}$ and $\theta_3^{(21)}$ are derived from the equations of the angular momenta of link 1 and link 2 about joint 1 and joint 2, respectively.

$$\begin{aligned}
&\frac{d}{dt}\left\langle \tilde{\rho}_c^{(1)T} v^{(1)} \right\rangle^{(1)} + \left\langle \tilde{\rho}_c^{(1)T} \tilde{\omega}^{(10)T} v^{(1)} \right\rangle^{(1)} \\
&\quad = -\tilde{r}_c^{(1)T} f^{(1)} - (\tilde{r}^{(1)T} - \tilde{r}_c^{(1)T}) A^{(12)} f^{(2)} \\
&\qquad + \tau^{(1)} - A^{(12)} \tau^{(2)} \qquad (9) \\
&\frac{d}{dt}\left\langle \tilde{\rho}_c^{(2)T} v^{(2)} \right\rangle^{(2)} + \left\langle \tilde{\rho}_c^{(2)T} \tilde{\omega}^{(20)T} v^{(2)} \right\rangle^{(2)} \\
&\quad = -\tilde{r}_c^{(2)T} f^{(2)} - (\tilde{r}^{(2)T} - \tilde{r}_c^{(2)T}) A^{(20)} f^{(e)} \\
&\qquad + \tau^{(2)} \qquad (10)
\end{aligned}$$

where,

$$\begin{aligned}
\rho_c^{(i)} &= \rho^{(i)} - r_c^{(i)} \\
r_c^{(i)} &= \frac{1}{m^{(i)}} \int \rho^{(i)} dm^{(i)} \\
< * >^{(i)} &= \int * dm^{(i)}
\end{aligned}$$

$m^{(i)}$ is mass of link i, $\boldsymbol{f}^{(i)} = [\boldsymbol{a}^{(i)}]^T f^{(i)}$ and $\boldsymbol{\tau}^{(i)} = [\boldsymbol{a}^{(i)}]^T \tau^{(i)}$ are a force and a torque acting on link i at joint i, and $\boldsymbol{f}^{(e)} = [\boldsymbol{a}^{(0)}]^T f^{(e)}$ is a force acting on the surface of the object through the end effector.
The torques $\tau^{(i)}$ $(i = 1, 2, 3)$ are divided into two parts.

$$\tau^{(i)} = \tau_d^{(i)} + \tau_{FB}^{(i)}$$

where $*_d$ indicates the desired feedforward torue and $*_{FB}$ feedback one.
The forces $f^{(1)}$ and $f^{(2)}$ are expressed as

$$\begin{aligned}
f^{(1)} &= \frac{d}{dt}\left\langle v^{(1)} \right\rangle^{(1)} + \tilde{\omega}^{(10)T} \left\langle v^{(1)} \right\rangle^{(1)} \\
&\qquad - m^{(1)} A^{(10)} g + A^{(12)} f^{(2)} \\
f^{(2)} &= \frac{d}{dt}\left\langle v^{(2)} \right\rangle^{(2)} + \tilde{\omega}^{(20)T} \left\langle v^{(2)} \right\rangle^{(2)} \\
&\qquad - m^{(2)} A^{(20)} g + A^{(20)} f^{(e)}
\end{aligned} \tag{11}$$

where g is a gravitational constant. The equations of motion for variables $\hat{w}_2^{(2)}$ are derived from the equations of elastic vibrations of link 2

$$\begin{aligned}
&\frac{d}{dt}\left\langle B^{(2)T} v^{(2)} \right\rangle^{(2)} + \left\langle B^{(2)T} \tilde{\omega}^{(20)T} v^{(2)} \right\rangle^{(2)} \\
&\quad = \left\langle B^{(2)T} \right\rangle^{(2)} A^{(20)} g - K^{(2)} \widehat{w}^{(2)} \\
&\qquad - 2\zeta^{(2)} \sqrt{< B^{(2)T} B^{(2)} >^{(2)} K^{(2)}}\ \dot{\widehat{w}}^{(2)} \\
&\qquad + E^{(2)T}(0) \tau^{(2)} + E^{(2)T}(R_1^{(2)}) \tau_d^{(3)} \qquad (12)
\end{aligned}$$

where, the second and third terms in the right hand side of Eq. (12) express an elastic restoring force and a structural damping force, respectively. The torque $\tau^{(3)}$ is divided into a passive compliance torque and an active control torque to control the force acting on the end effector. In Eq. (12), the passive torque $\tau_{FB}^{(3)}$ is included as a elastic restoring force of one finite element of link 2. On the other hand, the active control torque $\tau_d^{(3)}$ is included as the 5th term in the right hand side of Eq. (12).

$$\begin{aligned}
E^{(2)}(0) &= \begin{bmatrix} 0 & 0 & \cdots & 0 \\ 0 & 0 & \cdots & 0 \\ 1 & 0 & \cdots & 0 \end{bmatrix} \\
E^{(2)}(R_1^{(2)}) &= \begin{bmatrix} 0 & \cdots & 0 & 0 \\ 0 & \cdots & 0 & 0 \\ 0 & \cdots & 1 & 0 \end{bmatrix}
\end{aligned}$$

INVERSE MODEL

It is assumed that a desired trajectory $\boldsymbol{x}_d^{(e)}(t) = [\boldsymbol{a}^{(0)}]^T x_d^{(e)}$ of the end effector and a desired force $\boldsymbol{f}_d^{(e)}(t) = [\boldsymbol{a}^{(0)}]^T f_d^{(e)}$ acting on the surface of an object through the end effector are given. The inverse kinematics is to calculate the angles of rotation $\theta_{d3}^{(10)}(t)$ and $\theta_{d3}^{(21)}(t)$ and the elastic deformations $\widehat{w}_{d2}^{(2)}(t)$ corresponding to the desired trajectory and the desired force. First, the distance vector $\boldsymbol{x}^{(e)}$ of the end effector from joint 1 is expressed as

$$\begin{aligned}
\boldsymbol{x}^{(e)} &= [\boldsymbol{a}^{(0)}]^T x^{(e)} \\
x^{(e)} &= A^{(01)} r^{(1)} + A^{(02)} r^{(2)}
\end{aligned} \tag{13}$$

Substituting the desired trajectory $x_d^{(e)}$ into Eq. (13), we obtain the equation to determine the angles of rotation $\theta_{d3}^{(10)}$, $\theta_{d3}^{(21)}$.

$$\begin{aligned}
x_{d1}^{(e)} &= r^{(1)} \cos\theta_{d3}^{(10)} + r^{(2)} \cos\theta_{d3}^{(20)} \\
x_{d2}^{(e)} &= r^{(1)} \sin\theta_{d3}^{(10)} + r^{(2)} \sin\theta_{d3}^{(20)}
\end{aligned} \tag{14}$$

Next, substituting the desired force $f_d^{(e)}$ and the angles of rotation $\theta_{d3}^{(10)}$, $\theta_{d3}^{(21)}$ into Eq. (12) using Eq. (10), we obtain the equation to determine the elastic deformations $\widehat{w}_{d2}^{(2)}(t)$.

$$\begin{aligned}
&M^{(2)} \ddot{\widehat{w}}_{d2} + 2\zeta^{(2)} \sqrt{< B_2^{(2)T} B_2^{(2)} >^{(2)} K^{(2)}}\ \dot{\widehat{w}}_{d2}^{(2)} \\
&\quad + \left\{ K^{(2)} - \omega_{d3}^{(20)2} M^{(2)} \right\}\ \widehat{w}_{d2}^{(2)} \\
&= \Big(g_2 \cos\theta_{d3}^{(20)} - r_1^{(1)} \omega_{d3}^{(10)2} \sin\theta_{d3}^{(21)} \\
&\quad - r_1^{(1)} \dot{\omega}_{d3}^{(10)} \cos\theta_{d3}^{(21)} \Big) < B_2^{(2)T} >^{(2)} \\
&\quad - \dot{\omega}_{d3}^{(20)} < B_2^{(2)T} \rho_1^{(2)} >^{(2)} + \Big[< \rho_1^{(2)2} >^{(2)}\ \dot{\omega}_{d3}^{(20)}
\end{aligned}$$

$$
\begin{aligned}
&+m^{(2)} r_c^{(2)} \left\{ r^{(1)} \left(\cos\theta_{d3}^{(21)} \dot{\omega}_{d3}^{(10} + \sin\theta_{d3}^{(21)} \omega_{d3}^{(10)2} \right) \right. \\
&\left. + r_c^{(2)} \dot{\omega}_{d3}^{(20)} \right\} - m^{(2)} g_2 r_c^{(2)} \cos\theta_{d3}^{(20)} \\
&+ r^{(2)} f_{d2}^{(\epsilon)} \cos\theta_{d3}^{(20)} \Big] E_3^{(2)T}(0) \qquad (15) \\
M^{(2)} =& < B_2^{(2)T} B_2^{(2)} >^{(2)} - < B_2^{(2)T} C_2^{(2)} >^{(2)}
\end{aligned}
$$

where, $C_2^{(2)} = [\rho_1^{(2)},\ 0,\ \cdots,\ 0\ ]$. And the control torque $\tau_d^{(3)}$ is neglected in order to derive the inverse model.

Equation (15) is a set of second order ordinary differential equations and are appropriate to be formulated as initial value problem with the initial conditions

$$
t = 0, \qquad \hat{w}_2^{(2)} = \dot{\hat{w}}_2^{(2)} = 0
$$

However, since the coefficient matrix of $\ddot{\hat{w}}_{d2}^{(2)}$ is not positive definite, Eq. (15) are not well posed as initial value problems. Here, Eq. (15) are formulated as boundary value problems with the boundary conditions

$$
\begin{aligned}
t = 0 \qquad & \hat{w}_2^{(2)} = 0 \\
t = t_f \qquad & \hat{w}_2^{(2)} = 0
\end{aligned} \qquad (16)
$$

where, t_f is a time interval of manipulation.

As boundary value problems, we can obtain stable solutions numerically, but the elastic deformations $\hat{w}_{d2}^{(2)}$ obtained have certain velocities at the beginning of manipulation.

On the other hand, when the angle of rotation $\theta_{d3}^{(10)}(t)$ and $\theta_{d3}^{(21)}(t)$ and elastic deformations $\hat{w}_{d2}^{(2)}(t)$ are obtained, the inverse dynamics is to calculate the torques $\tau_d^{(1)}$ and $\tau_d^{(2)}$ which realize the desired motions. First, the variables $v_d^{(1)}$ and $v_d^{(2)}$ are calculated by using the variables $\theta_{d3}^{(10)}, \theta_{d3}^{(21)}$ and $\hat{w}_{d2}^{(2)}$

$$
\begin{aligned}
v_d^{(1)} &= \tilde{\rho}^{(1)} \omega_d^{(10)} \\
v_d^{(2)} &= A^{(21)} \tilde{r}^{(1)} \omega_d^{(10)} \\
&\quad + \omega_d^{(20)T} (\tilde{\rho}^{(2)} + B^{(2)} \hat{w}_d^{(2)}) + B^{(2)} \dot{\hat{w}}_d^{(2)}
\end{aligned} \qquad (17)
$$

Then, the forces $f_d^{(1)}(t)$ and $f_d^{(2)}(t)$ are calculated by using Eq. (11).

$$
\begin{aligned}
f_d^{(2)} &= \frac{d}{dt} \left\langle v_d^{(2)} \right\rangle^{(2)} + \tilde{\omega}_d^{(20)T} \left\langle v_d^{(2)} \right\rangle^{(2)} \\
&\quad - m^{(2)} A^{(20)} g + A^{(20)} f_d^{(\epsilon)} \\
f_d^{(1)} &= \frac{d}{dt} \left\langle v_d^{(1)} \right\rangle^{(1)} + \tilde{\omega}_d^{(20)T} \left\langle v_d^{(1)} \right\rangle^{(1)} \\
&\quad - m^{(1)} A^{(10)} g + A^{(12)} f_d^{(2)}
\end{aligned} \qquad (18)
$$

Finally, the torques $\tau_d^{(1)}$ and $\tau_d^{(2)}$ are calculated by substituting the variables $v_d^{(1)}$,$v_d^{(2)}$, $f_d^{(1)}$ and $f_d^{(2)}$ into the variables $v^{(1)}$, $v^{(2)}$, $f^{(1)}$ and $f^{(2)}$ in Eqs. (9),(10). But, the solutions $\tau_d^{(1)}$ and $\tau_d^{(2)}$ which satisfy Eqs. (9),(10) exactly do not exist and so, the solutions with the least squared errors are used as the models of the desired torques $\tau_d^{(1)}$ and $\tau_d^{(2)}$ as

$$
\begin{aligned}
\tau_d^{(2)} &= \frac{d}{dt} \left\langle \tilde{\rho}_c^{(2)T} v_d^{(2)} \right\rangle^{(2)} + \left\langle \tilde{\rho}_c^{(2)T} \tilde{\omega}_d^{(20)T} v_d^{(2)} \right\rangle^{(2)} \\
&\quad + \tilde{r}_c^{(2)T} f_d^{(2)} + \left(\tilde{r}^{(2)T} - \tilde{r}_c^{(2)T} \right) A^{(20)} f_d^{(\epsilon)} \\
\tau_d^{(1)} &= \frac{d}{dt} \left\langle \tilde{\rho}_c^{(1)T} v_d^{(1)} \right\rangle^{(1)} + \left\langle \tilde{\rho}_c^{(1)T} \tilde{\omega}_d^{(10)T} v_d^{(1)} \right\rangle^{(1)} \\
&\quad + \tilde{r}_c^{(1)T} f_d^{(1)} + \left(\tilde{r}^{(1)T} - \tilde{r}_c^{(1)T} \right) A^{(12)} f_d^{(2)} \\
&\quad + A^{(12)} \tau_d^{(2)}
\end{aligned} \qquad (19)
$$

The torques $\tau_d^{(1)}$ and $\tau_d^{(2)}$ are calculated by using elastic deformations $\hat{w}_{d2}^{(2)}$. Since elastic deformations $\hat{w}_{d2}^{(2)}$ have certain velocities at $t = 0$ and t_f. The torques $\tau_d^{(1)}$ and $\tau_d^{(2)}$ have impulsive components at $t = 0$ and t_f. This means that impulsive torques act on the system at the beginning of manipulation. The impulsive torque may excite higher modes of vibration which are not included in the inverse model, and this results in degradation of the performance of manipulation. Hence, the trajectory of the end effector must be designed not to excite the parasitic modes of vibration and this will be examined numerically in the following section.

NUMERICAL SIMULATION

Here, inverse models proposed in the previous section are verified numerically; The desired trajectory of the end effector $x_d^{(\epsilon)}$ and the desired force $f_d^{(\epsilon)}$ acting on the surface of the object are given and the torques $\tau_d^{(1)}$ and $\tau_d^{(2)}$ which realize the desired motion are calculated on the basis of the inverse models proposed. Then, the equations of motion of the manipulator are solved numerically where the torques obtained are used as the input torques, and the trajectory of the end effector $x^{(\epsilon)}$ and the force $f^{(\epsilon)}$ acting on the surface are compared with the desired trajectory of the end effector and the desired force acting on the surface. The values of parameters of the manipulator are listed in Table 1.

TABLE 1

	Link 1	Link 2
Length [m]	0.500	0.400
Mass [kg]	8.00	0.240
Bending Stiffness[Nm^2]	-	0.550
Damping Ratio	-	5.00 E-02

Natural Frequencies of link 2 are 2.4291 [Hz] (1st mode), 19.1016 [Hz] (2nd mode), 40.8210 [Hz] (3rd mode), 48.4743 [Hz] (4th mode), 115.7262 [Hz] (5th mode), 287.9078 [Hz] (6th mode), $\cdots$.
Link 2 is modeled as three finite elements for the inverse models ($N = 3$) including the rigid part and four finite elements for the numerical simulations ($N_{sim} = 4$) also including the rigid part of link 2; From 1st mode of vibration to 6th modes of vibration are included in inverse models, while from 1st mode of vibration to 8th mode of vibration are included in the models of simulation. The desired trajectory of the end effector and the desired force acting on the surface are given as follows,

$$\begin{aligned} x_{d2}^{(e)} &= 0.7 \quad [\mathrm{m}] \\ f_{d2}^{(e)} &= 2.0 \quad [\mathrm{N}] \end{aligned}$$

$$\begin{aligned} x_{d1}^{(e)} = 0.7 - 0.5(&-252\hat{t}^{11} + 1386\hat{t}^{10} - 3080\hat{t}^{9} \\ &+3465\hat{t}^{8} - 1980\hat{t}^{7} + 462\hat{t}^{6}) \quad [\mathrm{m}] \end{aligned}$$

where, $\hat{t} = t/t_f$.
The magnitudes of the velocities of the elastic deformations at the beginning of manipulation is proportional to the rates of acceleration of the end effector and so, in order to suppress the excitations of the modes of vibration, the end effector must be accelerated slowly.
Figure 2 shows the force acting on the surface of the object through the end effector. In figure 2, the impulsive torques are omitted.

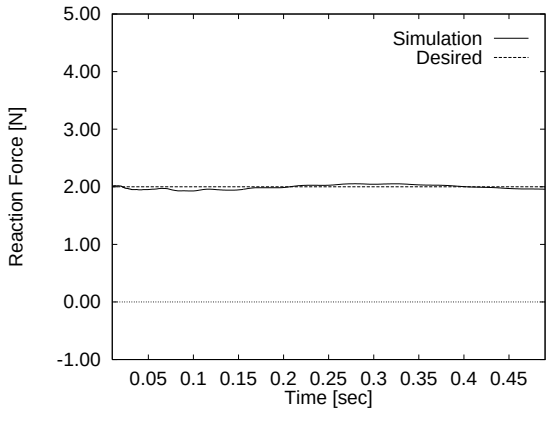

FIGURE 2: The force acting on the surface $t_f = 0.5$ [sec],without impulsive components

Figure 3 shows the difference between the desired forces $f_{d2}^{(e)}$ and the forces $f_2^{(e)}$ acting actually on the surface obtained by the numerical simulations as function of the time interval of manipulation t_f.

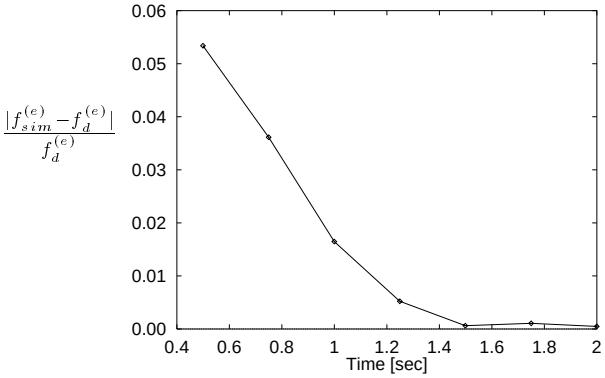

FIGURE 3: Difference between forces $f_d^{(e)}$ and $f_{sim}^{(e)}$ $t_f = 0.5$ [sec] without impulsive components

The figures show that the performances of manipulation are improved rapidly as the manipulator is accelerated slowly at the beginning of manipulation. Finally, figure 4 shows the stick diagrams of manipulator during manipulation

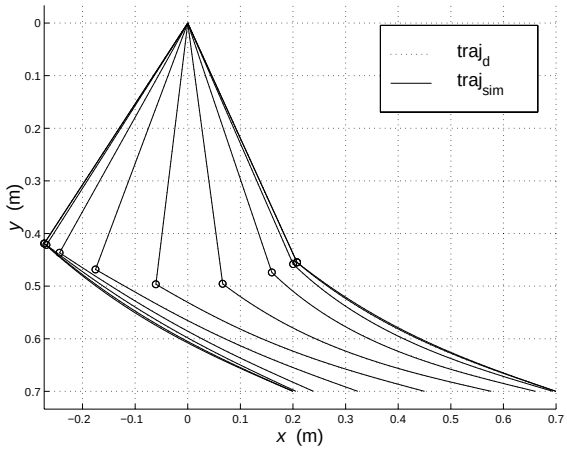

FIGURE 4: Stick diagram of the manipulator $t_f = 0.5$ [sec], without impulsive components

CONCLUSION

The models of the inverse kinematics and the inverse dynamics of a manipulator with elastic links for a trajectory and force control are derived. In the models, the equations for the elastic deformations of the elastic links are formulated as not initial value problems but boundary value problems. The elastic deformations obtained have velocities at the beginning and the end of manipulation and, as a result, the torques calculated include impulsive torques at the beginning and the end of manipulation. The models do not include any iteration processes. The performances of the proposed models are checked by the numerical simulations.

REFERENCES

1. Asada, H., Z.-D. Ma, and H. Tokumaru, "Inverse Dynamics of Flexible Robot Arms: Modeling and Computation for Trajectory Control," *ASME Journal of Dynamic Systems, Measurement, and Control*, 112, pp.177-185, 1990
2. Pfeiffer, F. " A Feedforward Decoupling Concept for the Control of Elastic Robots," Journal of Robotic Systems, Vol.6, No.4, 407-416, 1989
3. Kwon, D.-S., and Book, W.J.,"A Time-Domain Inverse Dynamics Tracking COntrol of a Single-Link Flexible Manipulator," Transactions of the ASME Journal of Dynamic Systems, Measurement, and Control, Vol. 116, pp.193-200, 1994
4. Bayo, E., P.Papadopoulos, J.Stubbe, and M.A.Serna, "Inverse Dynamics and Kinematics of Multi-link Elastic Robots: An Iterative Frequency Domain Approach," *International Journal of Robotics Research*,8(6), pp.49-62, 1989
5. Dai, Y.Q.,K.Usui, and M.Uchiyama, "A New Iterative Approach Solving Inverse Flexible-Link Manipulator Kinematics," *Proceedings of the 35th IEEE Conference on Decision and Control*, pp. 2493-2494, 1996

APPENDIX

Link 2 is divided into $N+1$ finite elements where are numbered as 1,2, $\cdots$,N from joint 2 to joint 3 and $N+1$ from joint 3 to the end effector. The nodes are also numbered as 0,1,$\cdots$,$N+1$ from joint 2 to the end effector. The model of an elastic deformation of the elastic part of link 2 is assumed as Euler-Bernoulli's beam model and the other rigid part of link 2 is used spring-mass system model. The deformation in element n,$w_{2,n}^{(2)}$ is expressed as

$$w_{2,n}^{(2)}(t,\rho_1^{(2)}) = \left[\begin{array}{cccc} \widehat{b}_{n-1} & \widehat{b}'_{n-1} & \widehat{b}_n & \widehat{b}'_n \end{array}\right] \left[\begin{array}{c} \widehat{w}_{2,n-1}^{(2)}(t) \\ \widehat{w}_{2,n-1}^{\prime(2)}(t) \\ \widehat{w}_{2,n}^{(2)}(t) \\ \widehat{w}_{2,n}^{\prime(2)}(t) \end{array}\right] \quad (20)$$

where, for $n = 1, \cdots, N$

$$\begin{aligned} \widehat{b}_{n-1} &= x_n^0 - \frac{3}{l^2}x_n^2 + \frac{2}{l^3}x_n^3\ , \quad \widehat{b}_n = \frac{3}{l^2}x_n^2 - \frac{2}{l^3}x_n^3 \\ \widehat{b}'_{n-1} &= x_n - \frac{2}{l}x_n^2 + \frac{1}{l^2}x_n^3\ , \quad \widehat{b}'_n = -\frac{1}{l}x_n^2 + \frac{1}{l^2}x_n^3 \\ x_n &= \left[\begin{array}{ll} 0 & ;0 < \rho_1^{(2)} < (n-1)l \\ \rho_1^{(2)} - (n-1)l & ;(n-1)l < \rho_1^{(2)} < nl \\ 0 & ;nl < \rho_1^{(2)} \end{array}\right] \\ l &= \frac{R_1^{(2)}}{N} \end{aligned}$$

for $n = N+1$

$$\begin{aligned} \widehat{b}'_{N+1} &= x_{N+1} - (r_1^{(2)} - R_1^{(2)}) \\ x_{N+1} &= \left[\begin{array}{ll} 0 & ;0 < \rho_1^{(2)} < R_1^{(2)} \\ \rho_1^{(2)} - R_1^{(2)} & ;R_1^{(2)} < \rho_1^{(2)} < r_1^{(2)} \\ 0 & ;r_1^{(2)} < \rho_1^{(2)} \end{array}\right] \end{aligned}$$

$\widehat{w}_{2,n}^{(2)}$: elastic deformation of element n at node n
$\widehat{w}_{2,n}^{\prime(2)}$: angle of rotation of element n at node n
At nodes 0 and $N+1$, we may set the condition that

$$\widehat{w}_0^{(2)} = \widehat{w}_{N+1}^{(2)} = 0$$

Then, an elastic deformation in link 2 is expressed as

$$w_2^{(2)}(t,\rho_1^{(2)}) = B^{(2)}(\rho_1^{(2)})\ \widehat{w}^{(2)}(t) \quad (21)$$

where,

$$B^{(2)} = \left[\begin{array}{c} 0 \\ B_2^{(2)} \\ 0 \end{array}\right]$$

$$B_2^{(2)} = \left[\begin{array}{cccccc} \widehat{b}'_0 & \widehat{b}_1 & \widehat{b}'_1 & \cdots & \widehat{b}_N & \widehat{b}'_N & \widehat{b}'_{N+1} \end{array}\right]$$

$$\widehat{w}^{(2)T} =$$

$$\left[\begin{array}{cccccccc} \widehat{w}_{2,0}^{\prime(2)} & \widehat{w}_{2,1}^{(2)} & \widehat{w}_{2,1}^{\prime(2)} & \cdots & \widehat{w}_{2,N}^{(2)} & \widehat{w}_{2,N}^{\prime(2)} & \widehat{w}_{2,N+1}^{\prime(2)} \end{array}\right]$$